REPUBLIC OF AZERBAIJAN

On the rights of the manuscript

ABSTRACT

of the dissertation for the degree of Doctor of Philosophy

DEVELOPMENT AND INVESTIGATION OF NEW TOPOLOGICAL INSULATOR MATERIALS BASED ON SYNTHETIC ANALOGUES OF NATURALLY OCCURRING MINERALS WITH TETRADYMITE-LIKE LAYERED STRUCTURES

Speciality: 2303.01 – Inorganic chemistry

Field of science: Chemistry

Applicant: **Fariz Aliyev Ramig**

Baku – 2024

The dissertation was carried out at the Department of "Chemistry and Technology of Inorganic Substances" of Azerbaijan State Oil and Industry University and at the "Inorganic Functional Materials" department of the Institute of Catalysis and Inorganic Chemistry named after Academician M. Nagiev of Ministry of Science and Education Republic of Azerbaijan

Scientific supervisor: D. Sci. Chem., associate professor
Dunya Mahammad Babanly

Official opponents: D. Sci. Chem., professor
İkhtiyar Bahram Bakhtiyarly

D. Sci. Chem., professor
Fuad Mikayil Sadiqov

Ph. D. Chem. associate professor
Vagif Gadir Valiyev

Dissertation Council ED 1.15 of Supreme Attestation Commission under the President of the Republic of Azerbaijan operating at the Institute of Catalysis and Inorganic Chemistry named after academician M.Nagiyev of the Ministry of Science and Education Republic of Azerbaijan

Chairman of the Dissertation Council:

D. Sci. Chem., Academician
Dilgam Babir Taghiyev

Scientific secretary of the Dissertation Council:

Ph. D. Chem., associate professor
Ulviyya Akhmed Mammadova

Chairman of the scientific seminar:

D. Sci. Chem., professor
Akif Shikhan Aliyev

GENERAL DESCRIPTION OF WORK

Relevance and Degree of Study of the Topic. The rapid advancement of contemporary science and technology has generated a significant demand for the exploration and synthesis of novel advanced materials that encompass unique physical properties. Therefore, scientific research dedicated to the prediction, targeted search, and design of innovative inorganic functional materials is of considerable importance.

One of the most significant inventions of our century is the new quantum state of matter known as the topological insulator (TI). This discovery has intensified research efforts in many leading scientific centers and modern research laboratories, particularly in the synthesis and design of new advanced functional materials. The primary characteristic that distinguishes TI materials from conventional conductors is their ability to function as insulators or semiconductors in the bulk while exhibiting conductive properties on their surfaces. These materials, characterized by a topological surface state, are considered to be the fundamental materials for devices and systems that can be applied in fields such as quantum computing, spintronics, optoelectronics, medicine, and etc. due to their unique properties.

Analysis of the scientific literature indicates that the compounds of the homologous series $(A^{IV}Te)_n(B_2^V Te_3)_m$ (A^{IV} = Ge, Sn, Pb; B^V = Sb, Bi) have consistently attracted attention of researchers as thermoelectric materials[1]. The thermal conductivity of such materials, characterized by a large elemental cage and heavy element atoms, is reduced due to the effective scattering of phonons, which in turn enhances thermoelectric efficiency. Recent studies suggest that these compounds also exhibit topological insulator properties. An effective approach in the search for such new materials involves the synthesis and investigation of phases with more complex compositions based on these compounds.

---

[1] Шелимова, Л. Е. Слоистые халькогениды в квазибинарных системах $A^{IV}B^{VI}$-$A^{V}{}_2B^{VI}{}_3$ (A^{IV}-Ge, Sn, Pb; B^V-Bi, Sb; B^{VI}-Te,Se) – перспективные термоэлектрические материалы для термогенераторов / Л.Е.Шелимова, О.Г.Карпинский, П.П.Константинов [и др] // Перспективные материалы, 2006. (3), - с. 5-17.

One of the fundamental and practically significant tasks in materials science is the development of new multicomponent inorganic materials and their requisite property sets. At the beginning of this century, the first studies on new high-entropy alloys (HEAs) began to be published. A key requirement for high-entropy polymetallic alloys is that they must consist of at least five main elements, with each element's proportion in the overall composition ranging from 5 to 35 atomic percent[2]. HEAs have garnered researchers' attention due to their promising characteristics, including high thermal, mechanical, and corrosion resistance, as well as ductility at cryogenic temperatures, superconductivity, and rich magnetic properties. Materials developed based on HEAs have a wide range of practical applications in fields such as medical biology, nuclear energy, tool manufacturing, aerospace research, hydrogen storage, and in the development of magnetic thin films and thermoelectric materials[3].

HEAs are usually composed of metallic components. However, these requirements are also met by multicomponent semiconductor phases, in particular, solid solutions of chalcogenides[4]. The study of chalcogenide type HEA plays important role in the design and optimization of thermoelectric materials.

Research Object and Subject. The objects of this dissertation research are the tetradymite-like layered compounds of the Ge-Bi-Te and Bi-Sb-Te-Se-S systems, with a specific focus on the compositional phase diagram of the Sb_2Te_2S-Sb_2Te_2Se-Bi_2Te_2Se-Bi_2Te_2S system. The subject of the research is the physicochemical investigation of these compounds and systems.

Objectives and Tasks of the Research. The aim of this scientific research is to determine the physicochemical interactions among the components in the $GeBi_2Te_4$-Bi_2, Sb_2Te_3-Sb_2S_3, and Sb_2Te_2S-Sb_2Te_2Se-

[2] Zhang, W. Science and technology in high-entropy alloys / W.Zhang, P.K.Liaw, Y.Zhang // Science. China Materials, - 2018. 61(1), - p. 2-22.

[3] Easo, P.G. High-entropy alloys / P.G.Easo, R.Dierk, O.R.Robert // Nature Reviews Materials, - 2019. 4(8), - p. 515-534.

[4] Jiang, B. High-entropy-stabilized chalcogenides with high thermoelectric performance / B.Jiang, Y.Yu, J.Cui [et al.] // Science. - 2021. 371(6531), - p. 830-834.

Bi_2Te_2Se-Bi_2Te_2S systems. This includes the identification of new phases, such as high-entropy alloys, as well as the determination of the thermodynamic and crystallographic parameters of certain phases.

Taking into account the above, the following **specific goals** were set and solved:

- The study of interactions in the $GeBi_2Te_4$-Bi_2 system, synthesis and crystallographic study of the obtained phases;
- Refinement of the phase diagram of the Sb_2Te_3-Sb_2S_3 system using a complex of modern physico-chemical research methods..
- The determination of the phase equilibrium in the five-component Bi-Sb-Te-Se-S system, specifically within the Sb_2Te_2S-Sb_2Te_2Se-Bi_2Te_2Se-Bi_2Te_2S compositional plane, employing by Differential Thermal Analysis (DTA), powder X-ray diffraction (PXRD), and Scanning Electron Microscopy with Energy Dispersive Spectroscopy (SEM-EDS). This includes the projection of its liquidus and solidus surfaces, as well as the construction of various boundary and internal polythermal sections of the phase diagram.
- The study of solid-phase equilibria and the thermodynamic properties of certain phases in the Sb_2S_3-Sb_2Te_3-Te-S system using the electromotive force (EMF) method.

Research Methods. The primary research methods employed in this dissertation include Differential Thermal Analysis (DTA), X-ray Powder Diffraction (XRD), Scanning Electron Microscopy (SEM), Energy Dispersive X-ray Spectroscopy (EDS), and electromotive force (EMF) techniques. DTA measurements were conducted using a multi-channel electronic data logger named "TC-08 Thermocouple Data Logger," as well as LINSEIS HDSC PT1600 and NETZSCH 404 F1 Pegasus devices. The powder X-ray diffraction patterns of the samples were recorded using a Bruker D2 PHASER diffractometer. During the analysis of the obtained X-ray diffraction patterns, the software programs Topas V4.2, Match!3, and FullProf Suite were utilized. The SEM-EDS analyses of the samples were performed using a Jeol-JSM 6700 F-Field Emission scanning electron microscope equipped with a Bruker Quantax EDS detector. EMF measurements were conducted using a Keithley 2100 6 1/2 digital multimeter.

Key Propositions for Defence

- The synthesis and characterization of new $GeBi_3Te_4$ and $GeBi_4Te_4$ compounds belonging to the homologous series $mGeBi_2Te_4$-nBi_2, along with data on their crystal structures and thermal stability.
- An updated phase diagram for the Sb_2Te_3-Sb_2S_3 system, detailing the melting characteristics and crystallographic parameters of the tetradymite-like Van der Waals type intermediate compound Sb_2Te_2S.
- Phase diagrams for the Sb_2Te_2S-Sb_2Te_2Se-Bi_2Te_2Se-Bi_2Te_2S compositional square of the Bi-Sb-Te-Se-S five-component system along the edges and some internal sections, including projections of the liquidus and solidus surfaces, as well as the crystallographic and thermal parameters of continuous solid solutions with cation and anion substitutions, including high-entropy phases.
- Results from the thermodynamic investigation of the Sb-Te and Sb_2S_3-Sb_2Te_3-Te-S systems using EMF measurements with a liquid electrolyte, including the standard integral thermodynamic functions of the existing binary and ternary phases.

Scientific Novelty of the Research

The dissertation presents the following new scientific results:

- New tetradymite-like layered structured compounds $GeBi_3Te_4$ and $GeBi_4Te_4$ were synthesized, formed by the alternating seven-layer $GeBi_2Te_4$ and two-layer Bi_2 packages. Their mono-crystals were grown and characterized using the Bridgman-Stockbarger method.
- The phase diagram of the Sb_2Te_3-Sb_2S_3 quasi-binary system was re-examined, resulting in a new version that differs from previously published literature. The presence of the Sb_2Te_2S compound with a tetradymite-type layered structure in the system has been confirmed, and its melting behavior has been determined.
- T-x phase diagrams for the Sb_2Te_2S-Sb_2Te_2Se-Bi_2Te_2Se-Bi_2Te_2S compositional square were constructed along the edges Sb_2Te_2S-Sb_2Te_2Se, Sb_2Te_2S-Bi_2Te_2S, Sb_2Te_2Se-Bi_2Te_2Se, and Bi_2Te_2S-Bi_2Te_2Se, demonstrating the existence of continuous solid solution series with cation and anion substitutions in these systems.
- High-entropy phases with tetradymite-like layered structures were obtained and characterized in the Sb_2Te_2S-Bi_2Te_2S-Bi_2Te_2Se-

Sb_2Te_2Se system.

- Projections of the liquidus and solidus surfaces of the Sb_2Te_2S-Bi_2Te_2S-Bi_2Te_2Se-Sb_2Te_2Se system were constructed, and analytical 3D modelling of these surfaces was conducted.
- Based on liquid electrolyte EMF measurements at temperatures ranging from 300 to 450 K, the partial molar functions of antimony in the Sb-Te system were calculated, along with the integral thermodynamic functions and standard entropy of the Sb_2Te_3 compound.
- The solid-phase equilibria of the Sb_2S_3–Sb_2Te_3–Te–S system were determined using XRD and EMF methods, and the integral thermodynamic functions of the Sb_2Te_2S compound and based on this, the integral thermodynamic functions of solid solutions have been calculated.

Theoretical and Practical Significance of the Research. The dissertation presents new scientific results concerning phase equilibria in the $GeBi_2Te_4$-Bi_2 and Sb_2Te_3-Sb_2S_3 sections, as well as the Sb_2Te_2S-Bi_2Te_2S-Bi_2Te_2Se-Sb_2Te_2Se compositional plane, along with the crystallographic and thermodynamic properties of newly identified phases. These findings contribute to the chemistry and materials science of layered structured complex chalcogenides. The results can be utilized in the directed synthesis of intermediate phases present in these systems and in the development of methodologies for growing monocrystals. It is noteworthy that the majority of the obtained phases are considered promising as thermoelectric materials, topological insulators, and materials possessing the properties of HEAs.

The potential for varying the composition across a broad range in the substitutional solid solutions, including HEAs, is significant. This variability facilitates the enhancement of the application properties of these phases.

The practical significance of this research also lies in the established new phase diagrams, as well as, the thermal, crystallographic, and thermodynamic properties of the compounds and solid solutions, which are important physicochemical parameters that can be included in various information databases.

The author has received 13 citations in the "Google Scholar Citations" information system for 4 scientific publications.

Approval and Application of the Work. The key results of this dissertation have been presented and discussed at the following scientific conferences: International Conference On Actual Problems Of Chemical Engineering Dedicate To The 100th Anniversary Of The Azerbaijan State Of Oil And Industry University (Baku, Azerbaijan 24-25.12.2020); 2nd International Science and Engineering Conference (Baku, Azerbaijan 26-27.11.2021); "Физико-химические процессы в конденсированных средах и на межфазных границах - Фагран-2021" (Voronezh, Russia 04-07.10.2021); XI Международная научная конференция "Кинетика и механизм кристаллизации. Кристаллизация и материалы нового поколения" (İvanova, Russia 20-24.09.2021); XVII International Freik Conference On Physics And Technology Of Thin Films And Nanosystems (Ivano-Frankivsk, Ukraine 11-16.10.2021); System. 6th Internatıanol Turkıc World Conference On Chemıcal Scıences And Technologıes (Baku, Azerbaijan 26-29.10.2022); Ümummilli Lider Heydər Əliyevin anadan olmasının 100-cü ildönümünə həsr olunmuş doktorant, magistrant və gənc tədqiqatçıların «Kimya və Kimya Texnologiyası» II Respublika Elmi Konfransı (Baku, Azerbaijan 04-05.05.2023); Ümummilli Lider Heydər Əliyevin anadan olmasının 100 illiyinə həsr olunmuş "Müasir təbiət ve iqtisad elmlərinin aktual problemləri" mözsunda beynalxalq elmi konfrans (Ganja, Azerbaijan 05-06.05.2023).

A total of 16 scientific publications have been produced on the dissertation topic, including 8 articles published in scientific journals (6 of which are indexed in Web of Science and Scopus). Additionally, 8 scientific works have been published as presentation abstracts at various international (7) and national (1) scientific conferences.

Name of the Organization Where the Dissertation Was Conducted. The dissertation was carried out at the Department of "Chemistry and Technology of Inorganic Substances" of Azerbaijan State Oil and Industry University and at the "Inorganic Functional Materials" department of the Institute of Catalysis and Inorganic Chemistry named after Academician M.Nagiev.

Overall Volume of the Dissertation with Individual Section Lengths. The dissertation comprises a total of 176 pages, including

an introduction (12,812 sign), four chapters (Chapter I - 47,483 signs, Chapter II - 41,117 signs, Chapter III - 38,863 signs, Chapter IV - 25,468 signs), main results (totally 168182 signs), a bibliography of 280 referenced works, and appendices. The dissertation contains 68 figures and 35 tables.

Author's Personal Contribution. The author played a leading role in formulating the research problem, developing the core ideas during the execution of the work, defining the directions of experimental investigations, conducting the experimental studies, and interpretation and generalization of the obtained results.

Acknowledgments. The author expresses deep gratitude to Prof. İmamaddin Amiraslanov (AR MSE Institute of Physics) and Assoc. Prof. Vagif Qasımov (AR MSE Institute of Catalysis and Inorganic Chemistry) for their assistance in conducting the XRD studies and for their valuable insights in interpretation of the obtained results.

MAIN CONTENTS OF THE WORK

The introduction provides the relevance of the dissertation, the object and subject of the study, the aims and objectives of the research, scientific novelty, practical significance, and the main propositions presented for defence.

In the first chapter of the dissertation, a literature review on the research objects is provided and analyzed. At the beginning of the chapter, information on the application properties of chalcogenides with a tetradymite-like layered structure is presented, and it is substantiated that these materials have the potential to be advanced functional materials for the future. Subsequently, the literature data on phase equilibria and the physico-chemical, crystallochemical, thermodynamic, and other properties of intermediate phases present in some binary and ternary systems have been collected and systematized in order to properly plan the experiments.

The second chapter provides information on the methods used in the preparation of the initial binary and ternary compounds that constitute the studied systems, as well as in the preparation of alloys with varying compositions of the research objects and the growth of

their single crystals. This chapter also includes a brief description of the physico-chemical analysis methods (DTA, XRD, EMF, SEM, and EDS) applied during the experimental investigations.

The initial binary and ternary compounds were synthesized by co-melting stoichiometric amounts of elements with high chemical purity (99.999%) from Alpha Aesar in quartz ampoules under vacuum conditions. The Sb_2S_3 compound, which is one of the initial components, was synthesized in a two-zone furnace, taking into account the high vapor pressure of sulfur. The synthesized samples were verified using DTA and XRD methods. The samples were prepared with a composition of 10-20 mol%, weighing between 0.5-1 gram. For synthesis, the initial binary and ternary compounds were loaded into quartz ampoules, sealed, and then synthesized in a one-zone furnace at temperatures ranging from 700-800 °C, depending on the composition of the sample. After the synthesis process, the alloys were quenched in ice water and thermally treated for 3-6 weeks at approximately 30-50 °C above the solidus line to achieve complete homogenization.

The third chapter presents and discusses the results obtained on phase equilibria in the Sb_2Te_3-Sb_2S_3 system and the Sb_2Te_2S-Bi_2Te_2S-Bi_2Te_2Se-Sb_2Te_2Se compositional square [5, 6, 9-15]. Additionally, new results are provided regarding the synthesis, thermal stability, and crystal structure of the $GeBi_4Te_4$ and $GeBi_3Te_4$ compounds in the Bi_2-$GeBi_3Te_4$ system [1, 2, 4, 7, 8].

The Sb_2S_3 – Sb_2Te_3 quasi-binary system [11, 15]. The X-ray diffraction patterns of samples with different compositions in the system are shown in Figure 1. As observed, the diffraction lines of the Sb_2S_3 and 10 mol% Sb_2Te_3 samples are similar, differing only by a slight shifting of the diffraction lines to small angles. Similarly, the diffraction pattern of the 90 mol% Sb_2Te_3 sample primarily consists of diffraction lines characteristic of a solid solution based on Sb_2Te_3. The diffraction patterns of samples containing 40, 60, 70, and 80 mol% Sb_2Te_3 indicate their non-homogeneity and the presence of a second phase. These diffraction patterns are composed of diffraction lines from two distinct phases, one of which is the Sb_2Te_2S (γ phase) compound. In addition to the γ phase, the diffraction patterns of the 40 and 60 mol% Sb_2Te_3-containing alloys also exhibit diffrac-

tion lines of the α phase based on Sb_2S_3, while the 70 and 80 mol% Sb_2Te_3-containing solids include diffraction lines of the β phase based on Sb_2Te_3. Analysis of the X-ray diffractogram of the sample with 66.7 mol% Sb_2Te_3 indicates that it is single-phase and corresponds to the Sb_2Te_2S compound with lattice parameters a = 4.1675 Å and c = 29.483 Å.

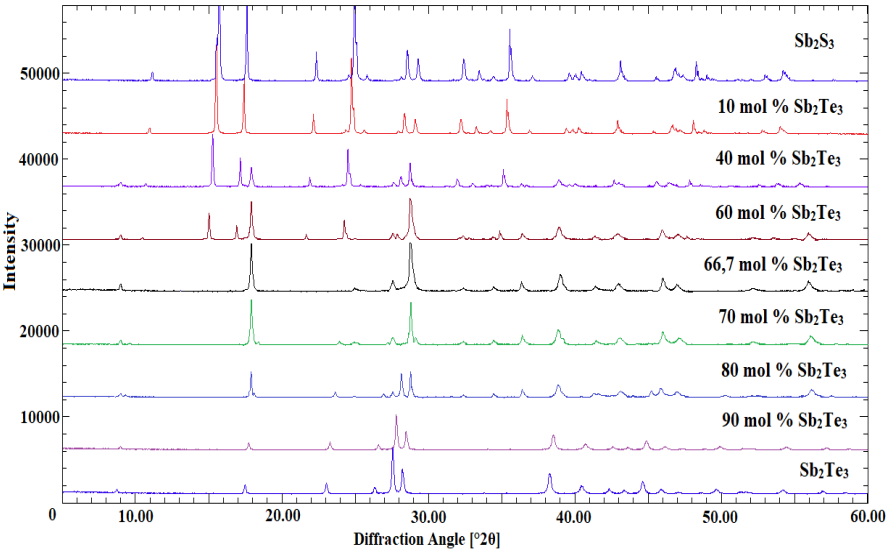

Figure 1. Powder diffraction patterns of the Sb_2Te_3-Sb_2S_3 system [15]

The constructed T-x phase diagram for the Sb_2S_3 – Sb_2Te_3 system is shown in Figure 2. As illustrated in the phase diagram, this quasi-binary system features a ternary compound that melts at 485 °C via a peritectic reaction: L + Sb_2Te_3(β) ↔ Sb_2Te_2S. The composition of the invariant peritectic point corresponds to 23 mol% (p) Sb_2Te_3. The system also possesses an eutectic point (e) located at 21 mol% Sb_2Te_3 and 475 °C. The ternary compound exhibits a very narrow initial crystallization field, making it quite challenging to obtain a pure crystal sample directly from its synthesis. The homogeneity range of this phase (γ phase) is approximately 66.7-69 mol% Sb_2Te_3. The system features 2 two-phase (α + γ and γ + β) and 2 single-phase homogeneous (α and β) regions based on the initial compounds.

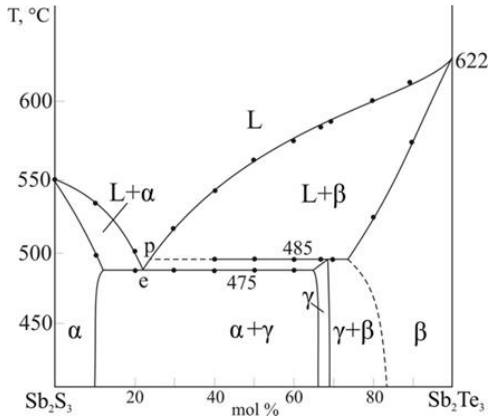

Figure 2. Phase diagram of the Sb_2S_3–Sb_2Te_3 system [15]

The two-phase region based on Sb_2S_3 (α phase) has been identified within the composition range of approximately 10-66.7 mol % Sb_2Te_3, while the two-phase region based on Sb_2Te_3 (β phase) spans approximately 69-83 mol% Sb_2Te_3.

Interactions between tetradymite and its analogs [5,6,9,10,12-14].

Structural analysis of tetradimite (Bi_2Te_2S) and other tetradimite-like compounds ($B^V_2Te_2X$ B^V = Sb, Bi; X= S, Se) indicates that the substitution of atoms (Te-Bi-S-Bi-Te) within the compound is feasible throughout all layers of its five-layered structure. For instance, tellurium atoms in the outer layers can be replaced by selenium and sulphur atoms, while sulphur atoms located in the central layers can be substituted with selenium and tellurium. Furthermore, substitution of Bi ↔ Sb in the outer layers is unrestricted. This scenario allows for the formation of continuous solid solutions within the concentration interval of Sb_2Te_2S-Sb_2Te_2Se-Bi_2Te_2Se-Bi_2Te_2S in the Bi-Sb-Te-Se-S five-component system, where substitutions occur in both cation and anion states.

This section discusses the results obtained regarding the synthesis and identification of five-component phases with a tetradimite-like structure in the Sb_2Te_2S-Sb_2Te_2Se-Bi_2Te_2Se-Bi_2Te_2S system.

The boundary sections of the Sb_2Te_2S-Sb_2Te_2Se-Bi_2Te_2Se-Bi_2Te_2S system [9, 13, 14].

The alloys of the Sb_2Te_2S-Bi_2Te_2S, Sb_2Te_2S-Sb_2Te_2Se, Sb_2Te_2Se-Bi_2Te_2Se, and Bi_2Te_2S-Bi_2Te_2Se systems subjected to thermal treatment were investigated using the XRD method. The results obtained for the first two systems are presented in Figure 3.

As shown in Figure 3, all alloys exhibited relevant anion and cation substitutions, resulting in diffraction patterns without any foreign phase mixtures, with peaks shifting slightly toward larger angles. This phenomenon is attributed to the formation of continuous solid solutions within the discussed system.

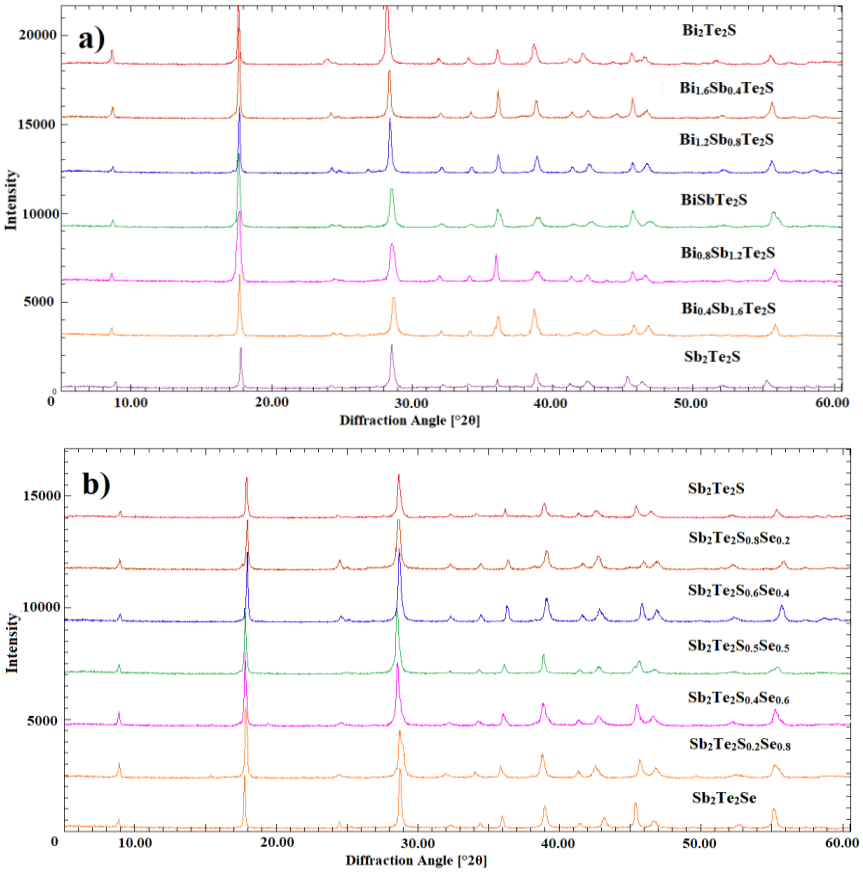

Figure 3. Powder diffraction patterns of the Sb_2Te_2S-Bi_2Te_2S (a) and Sb_2Te_2S-Sb_2Te_2Se (b) systems [9]

Figure 4a presents the phase diagram of the Sb_2Te_2S-Bi_2Te_2S system constructed based on the DTA results (Table 1). As seen in Figure 4a [14], the α-phase based on Sb_2Te_3 crystallizes from the liquid solution at <30 mol% Bi_2Te_2S. The crystallization of the α-phase below the liquidus continues in accordance with the monovariant peritectic reaction L + α ↔ γ, leading to the formation of an intermediate three-phase region L + α + γ that cannot be detected by DTA. Following the completion of the peritectic reaction, the residue of the alloy crystallizes to form the γ-phase. In regions with >30 mol% Bi_2Te_2S, the crystallization proceeds according to the L ↔ γ reaction, resulting in the formation of continuous solid solutions with Bi ↔ Sb cation substitutions. Throughout the entire concentration interval of the system, a continuous solid solution region of γ-phase exists below the solidus line.

Figure 4b presents the phase diagram constructed based on DTA results from the Sb_2Te_2S-Sb_2Te_2Se system. The incongruent melting of the Sb_2Te_2S compound leads to the crystallization of the α-phase based on Sb_2Te_3 in the concentration range of <20 mol% Sb_2Te_2Se from the melt.

Table 1

Differential thermal analysis (DTA) results and crystal lattice parameters of the $Sb_{2-x}Bi_xTe_2S$ alloys [14]

Composition, mol %	Thermal Effects, °C	Lattice constants, Å
Sb_2Te_2S	485, 580	*a = 4,1675(2), c = 29,483(1)*
10	497-518-575	---
20	510-551-571	*a = 4,1877(1), c = 29,503(2)*
30	525-568	---
40	539-576	*a = 4,2068(2), c = 29,527(3)*
50	560-590	*a = 4,2158(1), c = 29,530(3)*
60	566-600	*a = 4,2284(1), c = 29,548(2)*
70	581-605	---
80	595-610	*a = 4,2462(2), c = 29,569(3)*
90	605-617	---
Bi_2Te_2S	620	*a = 4,2648(1), c = 29,588(2)*

The subsequent crystallization of the α-phase results in the monovariant peritectic reaction L + α ↔ γ, which also contributes to

the formation of an intermediate three-phase region L + α + γ that cannot be recorded by DTA. In the concentration range of >20 mol% Sb_2Te_2Se, the crystallization process continues according to the L ↔ γ reaction. The system is characterized by the formation of a single-phase γ-phase below the solidus line, indicating the emergence of a continuous solid solution region due to S ↔ Se anion substitutions.

The T-x phase diagrams constructed based on DTA results for the Bi_2Te_2S-Bi_2Te_2Se [13] and Sb_2Te_2Se-Bi_2Te_2Se systems exhibit a relatively simple landscape characterized by direct crystallization of the γ-phase from the liquid (Figure 4c, d). Notably, the distinction between the Bi_2Te_2S-Bi_2Te_2Se system and the Sb_2Te_2Se-Bi_2Te_2Se system lies in the fact that in the first system, only one of the initial compounds (Bi_2Te_2Se) melts within the temperature range, whereas in the second system, both initial phases undergo melting within the same interval.

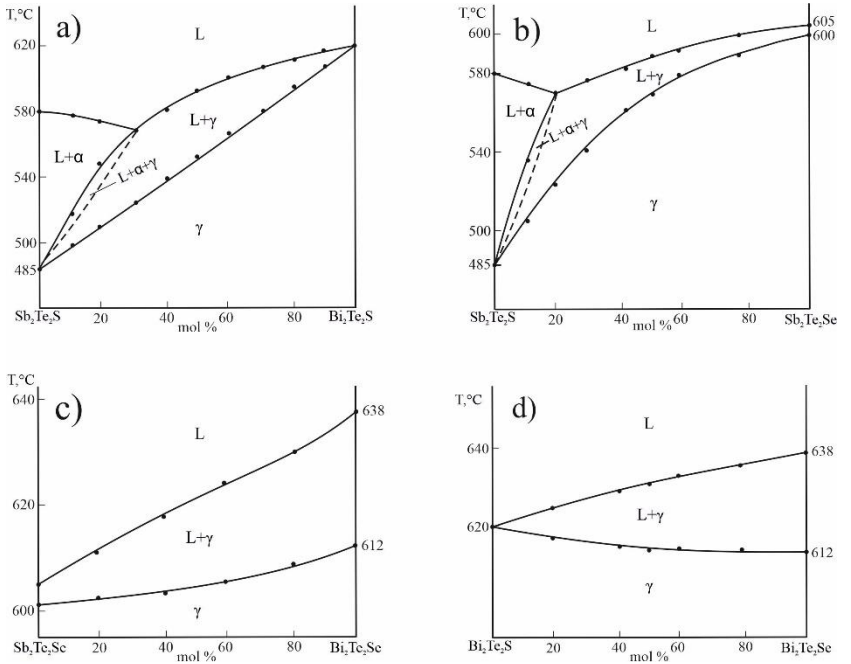

Figure 4. Phase diagram of the Sb_2Te_2S-Bi_2Te_2S(a), Sb_2Te_2S-Sb_2Te_2Se(b), Sb_2Te_2Se-Bi_2Te_2Se(c) and Bi_2Te_2S-Bi_2Te_2Se(d) systems [9]

Internal Sections of the Sb_2Te_2S-Sb_2Te_2Se-Bi_2Te_2Se-Bi_2Te_2S compositional square [5, 6, 9, 10, 12].

To investigate the crystallization process within the concentration square of the five-component system in more detail and to clarify the nature of the interactions between the components, the interaction characteristics of the components were studied along several internal polythermal sections, and the phase diagram of the respective systems was constructed.

This chapter presents new data on the synthesis and identifycation of five-component phases characterized by a tetradimite - like layered structure, which exhibit the properties of TIs within the Sb_2Te_2S-Bi_2Te_2S-Bi_2Te_2Se-Sb_2Te_2Se system. Single-phase alloys containing at least 5% elemental components within the concentration range of 25 mol% to 75 mol% can be classified as HEA. In the systems associated with internal sections, substitutions occurring in both cation and anion states are unrestricted. Therefore, the formation of continuous solid solutions in the studied systems is anticipated.

It should be noted that, while one of the initial compounds is Sb_2Te_2S, X-ray analysis of alloys with a composition of >70 mol% Sb_2Te_2S in the system reveals the presence of Sb_2Te_3 phase diffraction peaks in the powder diffraction patterns. Therefore, these samples were repressed into tablet form after synthesis and initial identification and subjected to thermal treatment at 450°C for approximately 500 hours. The XRD results of the additionally thermally treated tablets have proven that they are single-phase.

The powder X-ray diffraction analysis of the internal sections of the Sb_2Te_2S-Sb_2Te_2Se-Bi_2Te_2Se-Bi_2Te_2S system indicates (Figure 7) that all samples are qualitatively identical with no traces of any other phases present in the diffraction patterns. Furthermore, the successful attainment of stable single-phase solid solutions is one of the conditions necessary for HEA.

Figure 5 illustrates the compositional square of the Sb_2Te_2S-Bi_2Te_2S-Bi_2Te_2Se-Sb_2Te_2Se multicomponent system. The solid solutions within the green-highlighted internal square can be considered as HEA. These phases meet the general conditions applicable to this type of compound.

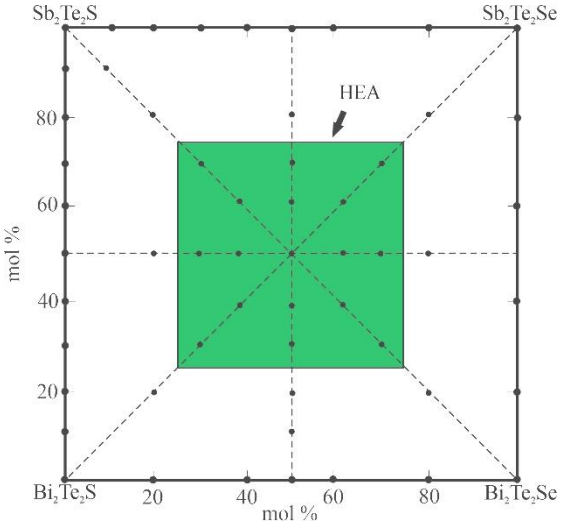

Figure 5. Composition square of the Sb_2Te_2S-Bi_2Te_2S-Bi_2Te_2Se-Sb_2Te_2Se system and the compositions of five-component alloys containing HEA properties. The black points show the compositions of investigated alloys [9]

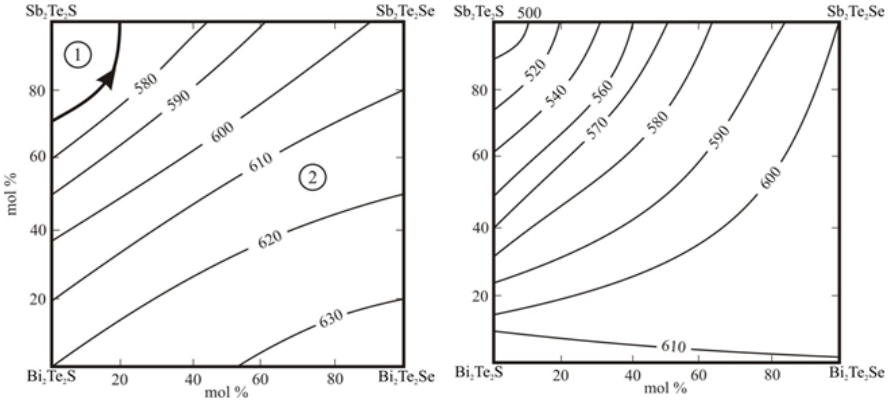

Figure 6. Projections of the liquidus (a) and solidus (b) surfaces of the Sb_2Te_2S-Bi_2Te_2S-Bi_2Te_2Se-Sb_2Te_2Se system. Primary crystallization fields: 1- α-phase; 2 - γ-phase [9]

The projections of the liquidus and solidus surfaces of the Sb_2Te_2S-Bi_2Te_2S-Bi_2Te_2Se-Sb_2Te_2Se system are shown in Figure 6. As observed, the liquidus surface consists of two regions corresponding to the initial crystallization of the α- and γ-phases. These surfaces

are separated by a peritectic curve representing the L + α ↔ γ multi-variant equilibrium. The solidus of the system corresponds to the completion of the crystallization of the γ-phase.

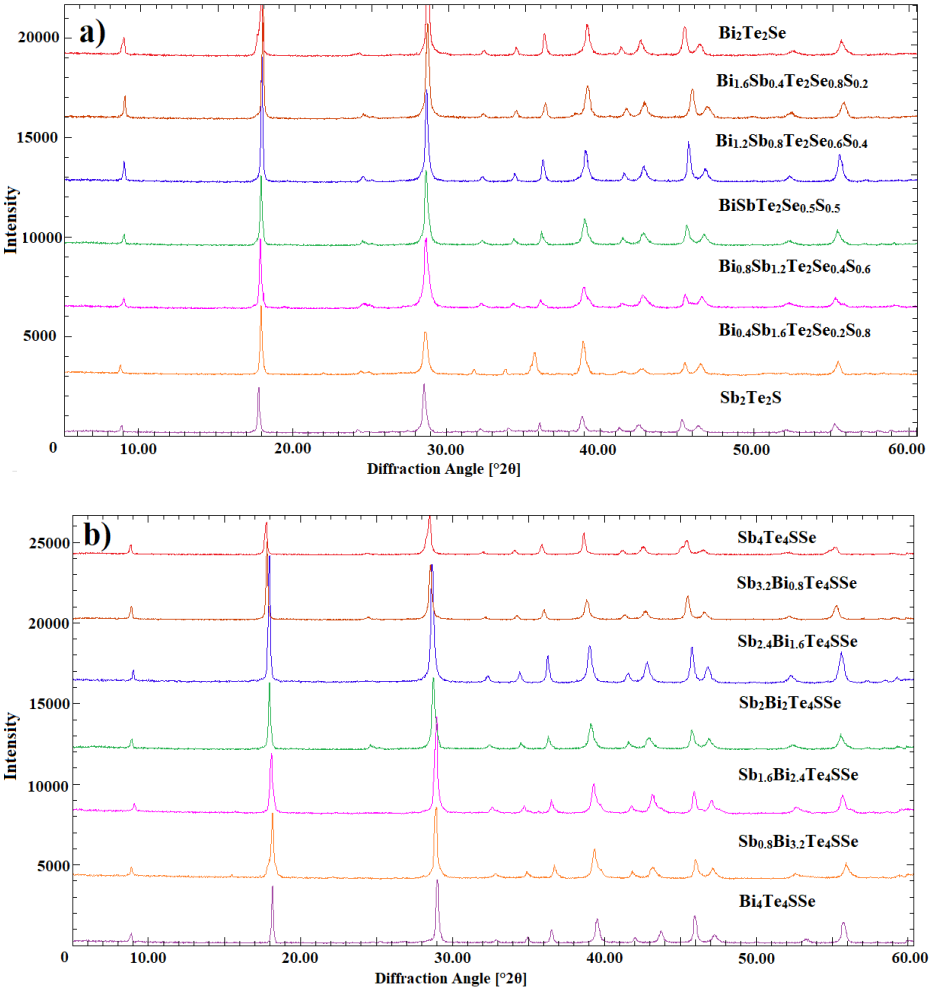

Figure 7. Powder diffraction patterns of Bi_2Te_2Se-Sb_2Te_2S(a), Sb_4Te_4SSe-Bi_4Te_4SSe(b) systems [9]

Figure 8a presents the T-x diagram for the Sb_2Te_2S-Bi_2Te_2Se [12] system. Due to the incongruent melting of the Sb_2Te_2S compound, the α-phase initially crystallizes from the liquid solution based on Sb_2Te_3 in the concentration range of <20 mol% Bi_2Te_2Se. As the temperature decreases, the crystallization of the α-phase passes to the monovariant peritectic reaction L + α ↔ γ. Consequently, an intermediate L + α + γ three-phase region emerges, which cannot be detected by means of DTA. In regions with >20 mol% Sb_2Te_2Se, the crystallization process proceeds according to the L ↔ γ reaction. In this region, a two-phase region L + γ arises between the liquidus and solidus curves. The formation of the γ-phase occurs below the solidus curve, which in turn results in the establishment of continuous solid solutions characterized by Sb ↔ Bi and S ↔ Se substitutions.

Table 2 presents the thermal effects and crystal lattice parameters for the samples of the Sb_2Te_2S-Bi_2Te_2Se system. Dependence of the lattice constants on composition for the Sb_2Te_2S-Bi_2Te_2S (Table 1) and Sb_2Te_2S-Bi_2Te_2Se (Table 2) systems are shown in Figure 9. As can be seen dependences are linear, obey Vegard's law, and proves the formation of continuous solid solutions.

As shown in Figures 8b, c, and d, the phase diagrams for all three systems are non-quasibinary due to the melting of one or both of the initial phases within the temperature range. The initial crystallization of the γ-phase in all three systems occurs from the L melt according to the L ↔ γ scheme. Below the solidus, the systems are stable and characterized by the formation of continuous solid solution regions. The obtained results can be utilized for the growth of monocrystals with the appropriate compositions.

Tables 1 and 2 present the DTA and XRD results for the Sb_2Te_2S -Bi_2Te_2S and Sb_2Te_2S-Bi_2Te_2Se systems. Graphs shown the dependency of lattice parameters on composition are shown in Figure 9. The dependence of lattice parameters on composition is linear and follows Vegard's law, indicating the formation of continuous solid solutions.

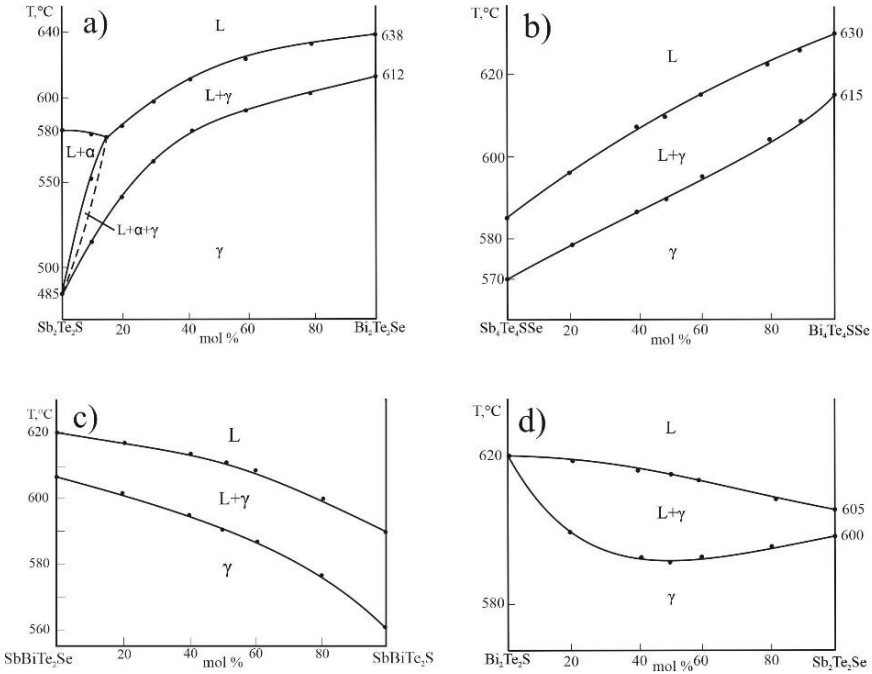

Figure 8. Phase diagram of the Bi_2Te_2Se-Sb_2Te_2S(a), Sb_4Te_4SSe-Bi_4Te_4Sse(b), $SbBiTe_2Se$-$SbBiTe_2S$(c) and Bi_2Te_2S-Sb_2Te_2Se(d) systems [9]

Table 2.

Differential thermal analysis (DTA) results and crystal lattice parameters of the Sb_2Te_2S-Bi_2Te_2Se system

Composition, mol %	Thermal Effects, °C	Lattice constants, Å
Sb_2Te_2S	485-580	*a*=4,1675(2), *c*=29,483(1)
20	542-582	*a*=4,1946(2), *c*=29,544(3)
40	580-623	*a*=4,2181(3), c=29,618(3)
50	592-610	*a*=4,2298(1), *c*=29,688(2)
60	594-619	*a*=4,2414(2), c=29,692(3)
80	605-629	*a*=4,2717(1), *c*=29,735(3)
Bi_2Te_2Se	612-638	*a*=4,2926(3), c=29,792(2)

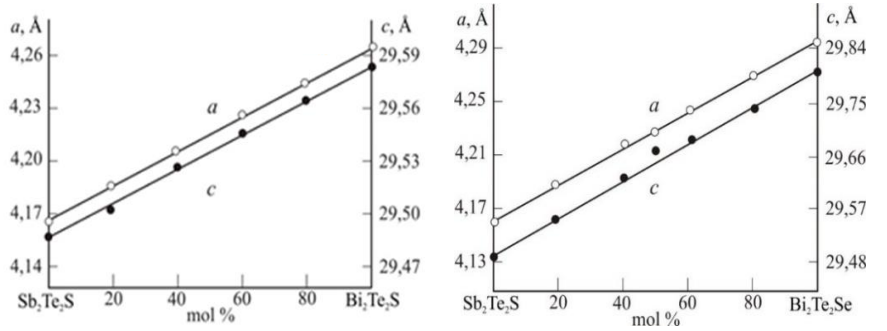

Figure 9. The composition dependencies of lattice constants of solid solutions along the Sb_2Te_2S-Bi_2Te_2S (a)[14] və Sb_2Te_2S-Bi_2Te_2Se (b) [14]

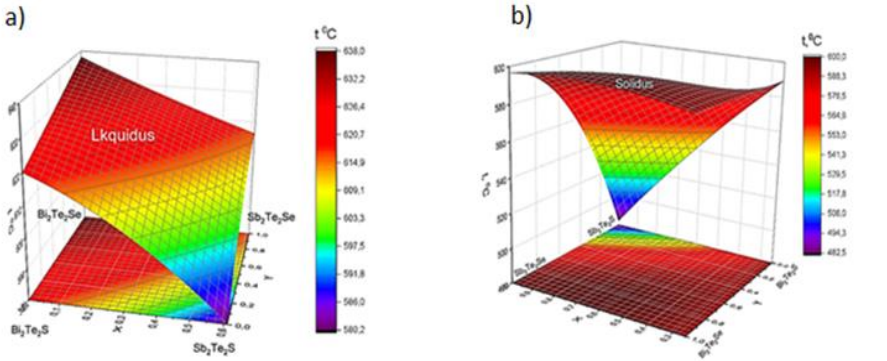

Figure 10. 3D view of the liquidus and the solidus surfaces of the Sb_2Te_2S-Bi_2Te_2S-Bi_2Te_2Se-Sb_2Te_2Se [9]

3D Modeling of the Liquidus and Solidus Surfaces of the Sb_2Te_2S-Bi_2Te_2S-Bi_2Te_2Se-Sb_2Te_2Se System [9].

This paragraph discusses the 3D modeling and representation of the Sb_2Te_2S-Bi_2Te_2S-Bi_2Te_2Se-Sb_2Te_2Se system using various equations. The modeling was conducted using the 3D analytical variant of the OriginLab software. Data obtained from the phase diagrams of the boundary sections of the system, as well as DTA results taken from various locations within the internal sections, were used to derive analytical expressions. The acquired data enable the 3D modeling of the liquidus and solidus surfaces of the Sb_2Te_2S-Bi_2Te_2S-Bi_2Te_2Se-Sb_2Te_2Se system (Figure 10).

Synthesis, Thermal Stability, and Crystal Structure of $GeBi_4Te_4$ and $GeBi_3Te_4$ Compounds [1, 2, 4, 7, 8]

The powder diffraction pattern of the $GeBi_4Te_4$ polycrystal is presented in Figure 11, compared with the diffraction patterns of elemental bismuth, $GeBi_2Te_4$, and $Ge_2Bi_2Te_5$ from the database. The diffraction pattern of the new phase was analysed and indexed using the TOPAS V3.0 software, identifying it as a new 9P-type tetradimite-like layered structure belonging to the ternary compound $GeBi_4Te_4$ (P3m1; a = 4.4071(6) Å, c = 17.384(2) Å).

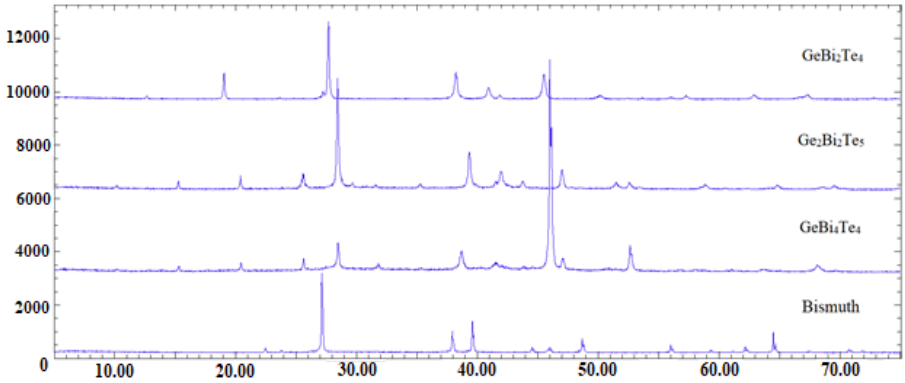

Figure 11. Comparison of the X-ray diffraction patterns of the $GeBi_4Te_4$, $GeBi_2Te_4$, $Ge_2Bi_2Te_5$ compounds, and elemental bismuth [2]

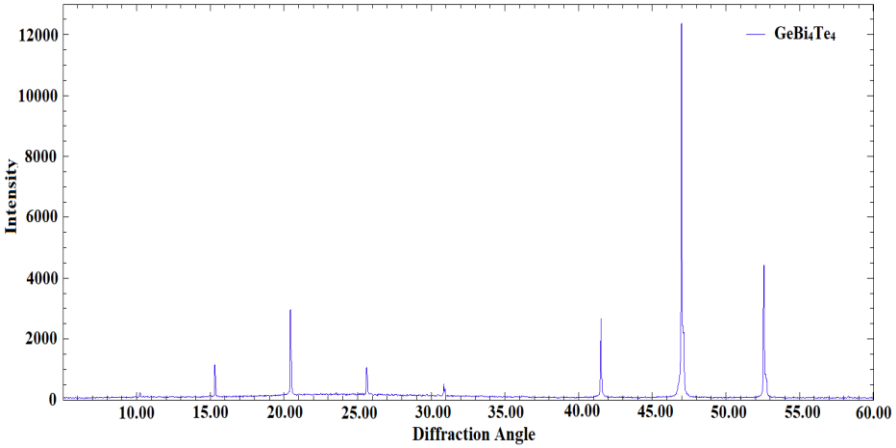

Figure 12. The X-ray diffraction pattern of the surface of a $GeBi_4Te_4$ single crystal grown using the Bridgman-Stockbarger method [2]

It is noteworthy that although the compositions and homologous series of the 9P-$GeBi_4Te_4$ and 9P-$Ge_2Bi_2Te_5$ compounds differ, both possess crystal structures composed of nine-layer packets. This results in closely similar c parameters, which is particularly evident in the overlap of diffraction lines at low angles.

A monocrystalline sample of $GeBi_4Te_4$ was grown from the liquid phase using the vertical Bridgman-Stockbarger method. The X-ray diffraction pattern of the sample obtained from the surface of the grown crystal that shown in Figure 12.

To determine the melting temperature and melting characteristics of the synthesized compound, samples were taken from various parts of the grown monocrystal, ground into powder, and subjected to DTA (Figure 13).

The first endothermic effect observed at 538°C is attributed to the peritectic decomposition of the $GeBi_4Te_4$ compound. The endothermic effect occurring at 563°C is believed to be related to the decomposition of another phase richer in germanium within the mBi_2-$nGeBi_2Te_4$ homologous series, which was not detected in the XRD analysis of the monocrystal's surface.

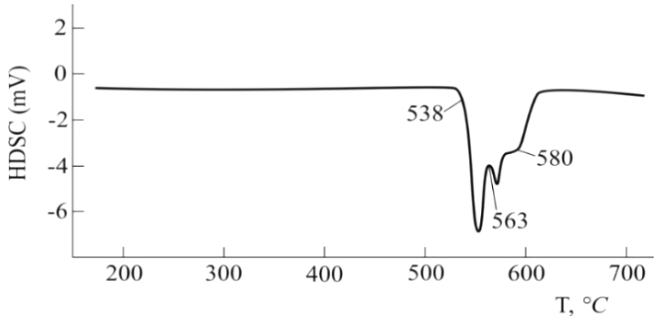

Figure 13. DTA heating thermogramme of the $GeBi_4Te_4$ phase [2]

The work also includes, XRD analysis of both polycrystalline and single crystals of the $GeBi_3Te_4$ compound [8]. The powder diffraction pattern of the polycrystalline sample was indexed as the $GeBi_3Te_4$ compound, with lattice parameters and space group determined as: a = 4.3625(5) Å, c = 31.381(2) Å, space group R3m1.

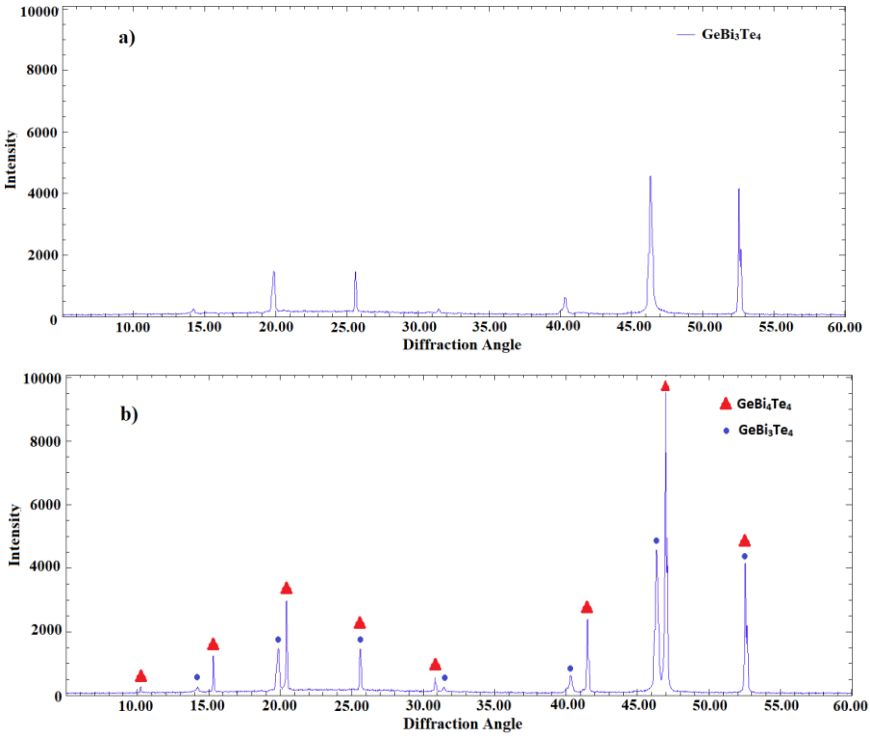

Figure 14. XRD pattern of a sample from the cleaved surface of the single-crystal a) $GeBi_3Te_4$, b) $GeBi_3Te_4$ + $GeBi_4Te_4$ [8]

DTA and XRD analyses were performed on a monocrystal of $GeBi_3Te_4$ grown by the Bridgman-Stockbarger method. Analysis of samples taken from various sections of the selected monocrystal revealed the presence of several phases (Figure 14). Based on XRD results, during the initial crystallization phase, a compound richer in germanium, $GeBi_3Te_4$, was identified from samples taken from the lower part of the monocrystal sample (Figure 14 a).

In contrast, samples taken from the relatively upper sections of the monocrystal revealed a mixture of two phases: $GeBi_3Te_4$ and $GeBi_4Te_4$ (Figure 14b). In the upper parts, i.e., in the last crystallized region, pure $GeBi_4Te_4$ phase is obtained. Research conducted on this single crystal has not revealed the presence of any other ternary mixed layered compounds.

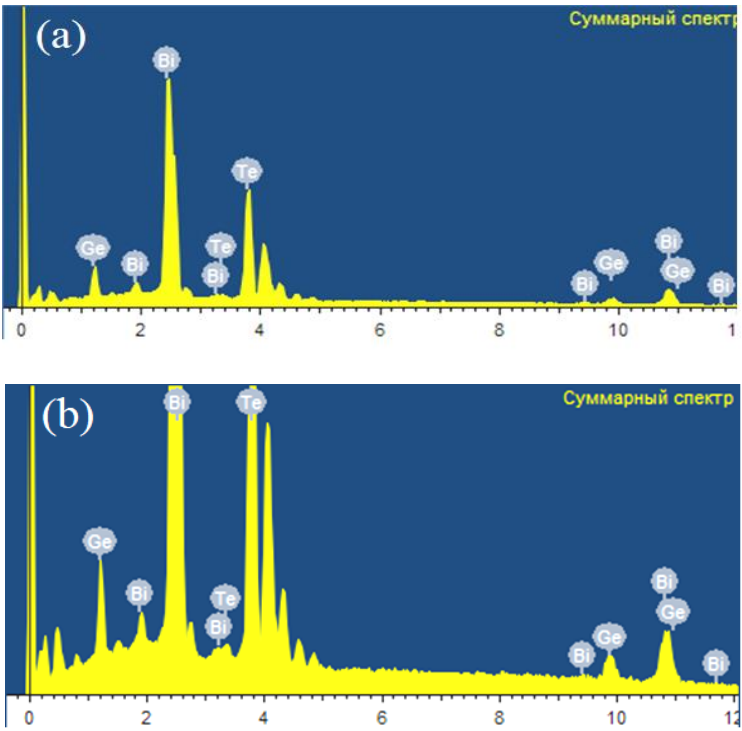

Figure 15. EDS spectrums of the $GeBi_4Te_4$ (a) and $GeBi_3Te_4$ (b) compounds

Table 3
The results of the elemental microanalysis of the $GeBi_4Te_4$ and $GeBi_3Te_4$ compounds

	Element	Mass %	Atom %	Error %
$GeBi_4Te_4$	Germanium - K	6.51	10.21	3.11
	Bismuth - M	56.31	46.17	1.41
	Tellurium - L	37.18	43.62	1.83
	Total	**100**	**100**	
$GeBi_3Te_4$	Germanium - K	6.38	14.74	3.42
	Bismuth - M	49.71	36.13	1.84
	Tellurium - L	44.35	49.13	1.47
	Total	**100**	**100**	

The results of the elemental analysis (EDS) for the $GeBi_4Te_4$ and $GeBi_3Te_4$ compounds are illustrated in Figure 15 and in Table 3.

A comparison of the EDS spectra of $GeBi_4Te_4$ and $GeBi_3Te_4$ indicates that the $GeBi_3Te_4$ ($2GeBi_2Te_4$–Bi_2) compound exhibits a higher intensity in the spectrum due to a richer presence of the elements germanium, bismuth, and tellurium.

At the beginning of the **fourth chapter**, the fundamental principles of the EMF method are discussed, along with several modifications used in thermodynamic research and the practical characteristics of applying the EMF method to heterogeneous systems. Additionally, the organization of experimental work using by EMF method, methodologies for processing results, and their execution are outlined. The subsequent sections present the results of investigations of the thermodynamic properties of binary and ternary phases formed in the Sb-Te-S system, as well as the solid solutions derived from these phases.

For the thermodynamic study of the Sb-Te and Sb-Te-S systems,

(–) Sb (b) | liquid electrolyte, Sb^{3+} | (Sb_2Te_3 + Te) (b) (+) (1)

(–) Sb (b) | liquid electrolyte, Sb^{3+} | Sb-S-Te (b) (+) (2)

electrochemical cells of the type mentioned were constructed to measure their EMF values in the temperature range of approximately 300-450 K [3, 16].

In both concentration cell, a glycerin solution was used as the electrolyte, and antimony as the active element of the system, was used as the solid electrode. As the right electrode, alloys of the Sb-Te system with 65 at.% Te and 75 at.% Te compositions were used in the (1) concentration cell, while in the (2) concentration cell, equilibrium samples taken from the Sb_2S_3-Sb_2Te_3-Te-S phase diagram of the solid-phase Sb-Te-S system were used.

The measurements have shown that the EMF values change linearly with temperature. As a result, it is also demonstrated that the EMF values remain stable within heterogeneous regions, while they change with a jump at the boundaries of these regions.

During measurements, it was established that the EMF values vary linearly with temperature. The results also indicate that EMF values remain stable within heterogeneous regions, changing only at the boundaries of these regions.

Two samples taken from the two-phase region of Sb_2Te_3+Te were used for the thermodynamic study of the Sb_2Te_3 compound. The linear temperature dependence of the EMF values allows the results to be processed using the least squares method in a computer program. As a result, the following types of linear equations were obtained:

$$E=a+bT\pm 2\cdot\left[(S_E^2/n)+S_b^2(T_i-\overline{T})^2\right]^{1/2} \quad (3)$$

here, *a* and *b* are the coefficients of the linear equation, n is the number of E and T value pairs, and $\overline{T}$ is the average temperature.

According to the linear equation (3):

$$E,\ mV = 102.03 + 0.0139 \pm 2\left[\frac{0.37}{30} + 1.3\cdot 10^{-5}\,(T - 351.39)^2\right]^{1/2} \quad (4)$$

obtained. Using the obtained equations of type (4) and the thermodynamic expressions provided below, the relative partial molar functions of antimony at 300 K have been calculated:

$$\Delta\bar{G}_{Sb} = -30.73 \pm 0.09\ \text{kC/mol}$$
$$\Delta\bar{H}_{Sb} = -29.53 \pm 0.49\ \text{kC/mol}$$
$$\Delta\bar{S}_{Sb} = 4.02 \pm 1.38\ \text{C/(K}\cdot\text{mol)}.$$

Based on the phase diagram of the Sb-Te system, these quantities represent the thermodynamic functions of the following virtual cell reaction.

$$2Sb(s.)+3Te(s.)=Sb_2Te_3(s.) \quad (5)$$

According to the reaction equation (5), the standard thermodynamic functions of formation Sb_2Te_3 compound were calculated using the following expressions [3]:

$$\Delta_f G^\circ_{Sb2Te3} = -61.46 \pm 0.18\ \text{kC / mol}$$
$$\Delta_f H^\circ_{Sb2Te3} = -59.06 \pm 0.98\ \text{kC / mol}$$
$$\Delta_f S^\circ_{Sb2Te3} = 8.04 \pm 2.76\ \text{C / mol}\cdot\text{K}$$

A comparative analysis of the obtained results indicates that the standard integral thermodynamic functions for the Sb_2Te_3 compound differ only slightly from values available in databases and reference books. The difference for $\Delta_f G^0$ is approximately 5-7%, for $\Delta_f H^0$ is about 4%, and for S° is only around 1-2%.

For the thermodynamic study of intermediate phases in the Sb-Te-S system, the final linear equations obtained by applying the least

squares method to various phase regions in the Sb_2S_3-Sb_2Te_3-Te-S [16] concentration field are presented in Table 4.

Sb_2S_3 is the only compound in the Sb-S binary system. Therefore, the partial molar functions of antimony in the Sb_2S_3 + S +Te phase field correspond to the

$$Sb\ (s.) + 1.5\ S\ (s.) = 0.5\ Sb_2S_3\ (s.) \quad (6)$$

potential-generating reaction. This reaction is similar to the reaction of formation of Sb_2S_3 compound from its elemental components. Therefore, the corresponding partial molar functions of antimony are thermodynamic functions of Sb_2S_3 formation for 1 g/at of antimony.

The standard integral thermodynamic functions of formation (Z ≡ G, H) and standard entropy of Sb_2S_3 were calculated using the following relations:

$$\Delta_f Z^0(Sb_2S_3) = 2\Delta\overline{Z_{Sb}} \quad (7)$$

$$S^0\ (Sb_2S_3) = 2\Delta\overline{S_{Sb}} + 2\ S^0(Sb) + 3\ S^0(S) \quad (8)$$

Table 4.
Equations of the temperature-dependent EMF of cells of the type (2) in some phase fields of the Sb_2S_3-Sb_2Te_3-Te-S system [16]

Phase field	$E = a \pm bT \pm 2S_E\ (T)$
Sb_2S_3+S+Te	$267.07 - 0.0505T \pm 2\ [\frac{0.93}{30} + 5.4 \cdot 10^{-5}\ (T - 340.2)^{\ 2}]^{1/2}$
Sb_2S_3+Sb_2Te_2S+Te	$180.96 - 0.0312T \pm 2\ [\frac{1.68}{30} + 3.8 \cdot 10^{-5}\ (T - 367.5)^{\ 2}]^{1/2}$
Sb_2Te_2S+β($Sb_2Te_{2.4}S_{0.6}$)+Te	$112.0 + 0.056T \pm 2\ [\frac{2.07}{30} + 2.1 \cdot 10^{-5}\ (T - 367.5)^{\ 2}]^{1/2}$
β ($Sb_2Te_{2.7}S_{0.3}$)+Te	$106.3 + 0.033T \pm 2\ [\frac{2.09}{30} + 4.8 \cdot 10^{-5}\ (T - 367.5)^{\ 2}]^{1/2}$

Table 5.
Partial molar functions of Sb in alloys of the Sb_2S_3-Sb_2Te_3-Te-S system(298 K) [16]

Phase field	$-\Delta\overline{G}_{Sb}$	$-\Delta\overline{H}_{Sb}$	$-\Delta\overline{S}_{Sb}$
	kJ·mole^{-1}		*J·mole^{-1}·K^{-1}*
Sb_2S_3+S+Te	71,50 ± 0,09	75,86 ± 0,72	-14,62±2,13
Sb_2S_3+Sb_2Te_2S+Te	49,69 ± 0,15	52,38 ± 0,66	-9,04±1,80
Sb_2Te_2S+β($Sb_2Te_{2.4}S_{0.6}$)+Te	37,25 ± 0,15	32,42 ± 0,75	16,21±2,02
β ($Sb_2Te_{2.7}S_{0.3}$)+Te	33,62 ± 0,15	30,77 ± 0,75	9,56±2,02

Taking into account the constancy of the compositions of the coexisting phases in the three-phase regions Sb_2S_3+Sb_2Te_2S+Te and Sb_2Te_2S+β($Sb_2Te_{2.4}S_{0.6}$)+Te, the standard integral thermodynamic properties of the Sb_2Te_2S compound and the limiting composition of beta-solid solutions ($Sb_2Te_{2.4}S_{0.6}$) were calculated by the method of potential-forming reactions. The partial molar functions of Sb in the above three-phase regions are thermodynamic functions of the following potential-forming reactions:

$$Sb+0{,}25\ Sb_2S_3+1{,}5\ Te=0{,}75\ Sb_2Te_2S \quad (9)$$

$$Sb+0{,}75\ Sb_2Te_2S+1{,}5\ Te=1{,}25\ Sb_2Te_{2{,}4}S_{0{,}6} \quad (10)$$

According to these reactions, the standard thermodynamic functions for the formation of ternary phases were calculated using

$$\Delta_f Z^0(Sb_2Te_2S)=1\frac{1}{3}\overline{\Delta Z}_{Sb}+\frac{1}{3}\Delta_f Z^0(Sb_2S_3) \quad (11)$$

$$\Delta_f Z^0(Sb_2Te_{2.4}S_{0.6})=0.8\overline{\Delta Z}_{Sb}+0.6\Delta_f Z^0(Sb_2Te_2S) \quad (12)$$

while their standard entropies were calculated using the expressions (13) and (14):

$$S^0(Sb_2Te_2S)=1\frac{1}{3}\overline{\Delta S}_{Sb}+1\frac{1}{3}S^0(Sb)+2S^0(Te)+\frac{1}{3}S^0(Sb_2S_3) \quad (13)$$

$$S^0(Sb_2Te_{2.4}S_{0.6})=0.8\overline{\Delta S}_{Sb}+0.8S^0(Sb)+1.2S^0(Te)+0.6S^0(Sb_2Te_2S) \quad (14)$$

Table 6.
Standard integral thermodynamic functions of the phases in the Sb–S–Te system

Phase field	$-\Delta\bar{G}_{Sb}$	$-\Delta\bar{H}_{Sb}$	$\Delta_f S^0$	S^0
	kJ·mole^{-1}		*J·mole*$^{-1}$·*K*$^{-1}$	
Sb_2S_3	143,0±0,2	151,7±1,5	-29,2±4,3	157,7±5,9
Sb_2Te_2S	113,9±0,3	120,4±1,4	-21,9±3,7	200,2±5,5
β($Sb_2Te_{2,4}S_{0,6}$)	98,1±0,4	98,2±1,1	-0,3±3,8	228,9±5,7
β($Sb_2Te_{2,7}S_{0,3}$)	82,7±0,4	79,9±1,3	9,4±4,0	243,8±6,1
Sb_2Te_3	64,46±0,18	59,06±0,98	8,0±2,8	247,5±4,4

The calculation of the standard thermodynamic functions of the formation of β-solid solutions of the $Sb_2Te_{2,7}S_{0,3}$ composition was carried out by graphical integration of the Gibbs-Duhem equation along the Sb_2Te_3-Sb_2S_3 section according to the well-known method. The obtained results are presented in Table 6.

The results for Sb_2S_3 show minimal deviation from the recommended in the literature values. The thermodynamic functions for solid solutions based on tetradimite with compositions of $Sb_2Te_{2.4}S_{0.6}$ and $Sb_2Te_{2.7}S_{0.3}$ have been determined for the first time in this study.

RESULTS

1. The systems $GeBi_2Te_4$-Bi_2, Sb_2Te_3-Sb_2S_3, and the five-component Bi-Sb-Te-Se-S system, specifically the Sb_2Te_2S-Sb_2Te_2Se-Bi_2Te_2Se-Bi_2Te_2S concentration plane, were comprehensively investigated using DTA, XRD, and SEM-EDS methods. The nature of the physical-chemical interactions between components was established, and phase diagrams were constructed.
2. New mixed-layer tetradimite-like compounds $GeBi_3Te_4$ and $GeBi_4Te_4$ were discovered, formed by the alternation of seven-layer $GeBi_2Te_4$ and two-layer Bi_2 packets. These compounds were synthesized individually and identified using various physical-chemical analytical methods. XRD analysis revealed that the crystal structure of the identified ternary compounds consists of a repetition of seven-layer Te-Bi-Te-Ge-Te-Bi-Te ($GeBi_2Te_4$) and two-layer Bi-Bi packets along the c-axis. The crystal lattice parameters of the obtained compounds were determined using the Rietveld method based on powder X-ray diffraction data [1,2,4,7,8].
3. The phase diagram of the quasi-binary Sb_2S_3-Sb_2Te_3 system was re-examined, resulting in a novel variant that differs from the eutectic-type phase diagram found in the literature. In this newly presented phase diagram, the presence of the tetradimite-like layered compound Sb_2Te_2S, which exhibits incongruent melting and a very small initial crystallization region, was identified, marking a significant deviation from previous studies[11,15].
4. The concentration square of the five-component Bi-Sb-Te-Se-S

system was analysed for the Sb_2Te_2S-Sb_2Te_2Se-Bi_2Te_2Se-Bi_2Te_2S compositions, establishing phase equilibria across various boundaries and internal sections, including Sb_2Te_2S-Bi_2Te_2S, Sb_2Te_2S-Sb_2Te_2Se, Sb_2Te_2Se-Bi_2Te_2Se, and Bi_2Te_2S-Bi_2Te_2Se. Continuous solid solutions resulting from cation (Bi ↔ Sb) and anion (S ↔ Se) substitutions were confirmed. Projections of the liquidus and solidus surfaces for the Sb_2Te_2S-Sb_2Te_2Se-Bi_2Te_2Se-Bi_2Te_2S system were constructed, and their analytical 3D modelling was performed [5,6,9,10,12,13,14].

5. The standard formation Gibbs free energy, enthalpy, and entropy of the Sb_2Te_3 compound were calculated using the electrochemical measurement technique for the standard electromotive force in the temperature range of 300-450 K with respect to the stibium electrode [3].
6. By utilizing XRD and EMF measurements of the concentration elements in relation to the stibium electrode, a solid-phase equilibrium diagram for the Sb-Te-S ternary system within the Sb_2S_3-Sb_2Te_3-Te-S concentration range at 300 K was constructed. Based on the EMF measurements, the standard formation thermodynamic functions and standard entropies of the Sb_2S_3 and Sb_2Te_2S compounds, as well as solid solutions of $Sb_2Te_{2.4}S_{0.6}$ and $Sb_2Te_{2.7}S_{0.3}$ derived from Sb_2Te_2S, were determined [16].

THE MAIN RESULTS OF THE WERE PUBLISHED IN THE FOLLOWING SCIENTIFIC WORKS:

1. Aliyev, F.R., Orujlu, E.N., Amiraslanov, I.R., Babanly, D.M. A New 9P–Type Layered van der WAALS phase – $GeBi_4Te_4$ in the Ge-Bi-Te system // International Conference on Actual Problems of Chemical Engineering, Dedicate to The 100th Anniversary Of The Azerbaijan State Of Oil And Industry Universit, -Baku: - 2020. – p. 112-113.
2. Aliyev, F.R. Synthesis and Study of a Novel 9P-type Mixed Layered Tetradymite-Like $GeBi_4Te_4$ Compound in the Ge-Te-Bi System // Physics and Chemistry of Solid State, - Ivano-Frankivsk: – 2021. 22(3), - p. 401-406.

3. Aliyev, F.R.Thermodynamic properties of the Sb_2Te_3 compound / F.R.Aliyev, E.N.Orujlu, D.M.Babanly // Azerbaijan Chemical Journal, - Baku: - 2021. (4), - p. 53-59.
4. Aliyev, F.R., Babanly, D.M. Synthesis and Characterization of New Mixed Layered Compounds In The nBi_2 – $mGeBi_2Te_4$ Homologous Serie // 2nd İnternational Science and Engineering Conference, - Baku: - 2021. – p. 252-255.
5. Алиев, Ф.Р., Имамалиева, С.З., Бабанлы, Д.М. Высокоэнтропийные сплавы в системе Sb-Bi-S-Se-Te // "Физико-химические процессы в конденсированных средах и на межфазных границах", Воронеж – 2021. – с. 166-167.
6. Алиев, Ф.Р., Имамалиева, С.З., Салимов, З.Э., Бабанлы, Д.М. Высокоэнтропийные сплавы со структурой тетрадимита // XI Международная научная конференция "Кинетика и механизм кристаллизации. Кристаллизация и материалы нового поколения",Иваново, - 2021. – с. 227-228.
7. Aliyev, F.R., Babanly, D.M. Synthesis and characterization of new mixed layered compounds $GeBi_3Te_4$ and $GeBi_4Te_4$ // XVII International Freik Conference On Physics And Technology Of Thin Films And Nanosystems, - Ivano-Frankivsk: - 2021. – p. 77.
8. Aliyev, F.R. Synthesis and study of a new mixed-layered compound $GeBi_3Te_4$ belonging to the nBi_2–$mGeBi_2Te_4$ homologous series / F.R.Aliyev, E.N.Orujlu, D.M.Babanly // Bulletin of the University of Karaganda – Chemistry, - Karaganda: - 2022. 105(1), - p. 92-98.
9. Aliyev, F.R. Layered High-Entropy Alloys Based on Antimony and Bismuth Chalcogenides / F.R.Aliyev, D.M.Babanly, I.R.Amiraslanov [et al.] // Nova Science Publishers Properties and Uses of Antimony, - New-York: - 2021. – p. 73-95.
10. Aliyev, F.R. The $SbBiTe_2Se$-$SbBiTe_2S$ phase diagram of the Sb-Bi-S-Se-Te system // Azerbaijan Journal of Chemical News, - Baku: 2022. 4(1), - p. 6-12.
11. Aliyev, F.R., Babanly D.M. Phase Relations in The Sb_2Te_3-Sb_2S_3 // System. 6th Internatianol Turkic World Conference on Chemical Sciences and Technologies, - Baku: – 2022. – p. 71.

12. Aliyev, F.R., Ahmadov, E.J., Babanly, D.M., Bayramova, A.Q. Phase Relations in the Sb_2Te_2S-Bi_2Te_2Se // Ümummilli Lider Heydər Əliyevin anadan olmasının 100 illiyinə həsr olunmuş "Müasir təbiət ve iqtisad elmlərinin aktual problemləri" məzsunda beynalxalq elmi konfrans, - Gəncə: - 2023. – s. 20-21.
13. Aliyev, F., Jafarov, Y., Babanly, M. Phase Equilibria İn The Bi_2Te_2S – Bi_2Te_2Se System // Ümummilli Lider Heydər Əliyevin anadan olmasının 100-cü ildönümünə həsr olunmuş doktorant, magistrant və gənc tədqiqatçıların «Kimya və Kimya Texnologiyasi» II Respublika Elmi Konfransının, - Bakı: – 2023. - p 184-185.
14. Aliyev, F.R. Phase Relations in the Sb_2Te_2S-Bi_2Te_2S System and Characterization of $Sb_{2-X}Bi_xTe_2S$ Solid Solutions / F.R.Aliyev, E.N.Orujlu, D.M.Babanly [et al.] // Chemical Problems, - Baku: – 2023. 2 (21) - p. 132-139.
15. Aliyev, F.R. An Update Phase Diagram of The Sb_2Te_3-Sb_2S_3 System / F.R., Aliyev, E.N., Orujlu, G.B., Dashdiyeva [et al.] // New Materials, Compounds and Applications, - Baku: – 2023. 2(7), - p.76-83.
16. Aliyev, F.R. Solid – phase equilibria and thermodynamic properties of the Sb-Te-S system / F.R.Aliyev, E.N.Orujlu, L.F.Mashadiyeva [et al.] // Physics and Chemistry of Solid State, - Ivano-Frankivsk: – 2024. 25(1), - p. 26-34.

The defense will be held on 16 January 2025 at 10^{00} at the meeting of the Dissertation council ED1.15 of Supreme Attestation Commission under the President of the Republic of Azerbaijan operating at the Institute of Catalysis and Inorganic Chemistry named after acad. M. Nagiyev of the Ministry of Science and Education of the Republic of Azerbaijan

Address: H.Javid, 113, AZ-1143, Baku, Azerbaijan
E-mail: kqki@kqki.science.az

The dissertation is available in the library of the Institute of Catalysis and Inorganic Chemistry named after acad. M.Naghiyev of the Ministry of Science and Education of the Republic of Azerbaijan.

Electronic versions of dissertation and its abstract are available on the official website of the Institute of Catalysis and Inorganic Chemistry named after academician M.Naghiyev of the Ministry of Science and Education of the Republic of Azerbaijan www.kqkiamea.az

Abstract was sent to the required addresses on 13 December 2024

Signed for print: 05.12.2024

Paper format: 60x84$^{1/16}$

Volume: 38 005 characters

Number of hard copies: 20